HHS Public Access

Author manuscript

Adv Ther (Weinh). Author manuscript; available in PMC 2021 April 13.

Published in final edited form as:

Adv Ther (Weinh). 2019 April ; 2(4): . doi:10.1002/adtp.201800139.

A Viral Nanoparticle Cancer Vaccine Delays Tumor Progression and Prolongs Survival in a HER2+ Tumor Mouse Model

Sourabh Shukla[*]

Department of NanoEngineering, University of California San Diego, La Jolla, CA 92093, USA

Department of Biomedical Engineering, Case Western Reserve University, 10900 Euclid Avenue, Cleveland, OH 44106, USA

Case Comprehensive Cancer Center, Case Western Reserve University, 10900 Euclid Avenue, Cleveland, OH 44106, USA

Michal Jandzinski

Department of Biomedical Engineering, Case Western Reserve University, 10900 Euclid Avenue, Cleveland, OH 44106, USA

Chao Wang

Department of NanoEngineering, University of California San Diego, La Jolla, CA 92093, USA

Department of Biomedical Engineering, Case Western Reserve University, 10900 Euclid Avenue, Cleveland, OH 44106, USA

Case Comprehensive Cancer Center, Case Western Reserve University, 10900 Euclid Avenue, Cleveland, OH 44106, USA

Xingjian Gong

Department of Biomedical Engineering, Case Western Reserve University, 10900 Euclid Avenue, Cleveland, OH 44106, USA

Kristen Weber Bonk

Case Comprehensive Cancer Center, Case Western Reserve University, 10900 Euclid Avenue, Cleveland, OH 44106, USA

Department of Pharmacology, Case Western Reserve University, 10900 Euclid Avenue, Cleveland, OH 44106, USA

Ruth A. Keri

Case Comprehensive Cancer Center, Case Western Reserve University, 10900 Euclid Avenue, Cleveland, OH 44106, USA

Department of Pharmacology, Case Western Reserve University, 10900 Euclid Avenue, Cleveland, OH 44106, USA

[*] sshukla@eng.ucsd.edu; nsteinmetz@ucsd.edu.

Supporting Information

Supporting Information is available from the Wiley Online Library or from the author.

Conflict of Interest

The authors declare no conflict of interest.

Nicole F. Steinmetz*

Department of NanoEngineering, University of California San Diego, La Jolla, CA 92093, USA

Department of Biomedical Engineering, Case Western Reserve University, 10900 Euclid Avenue, Cleveland, OH 44106, USA

Case Comprehensive Cancer Center, Case Western Reserve University, 10900 Euclid Avenue, Cleveland, OH 44106, USA

Department of Bioengineering, University of California San Diego, La Jolla, CA 92093, USA

Department of Radiology, University of California San Diego, La Jolla, CA 92093, USA

Moores Cancer Center, University of California San Diego, La Jolla, CA 92093, USA

Abstract

Human epidermal growth factor receptor 2 (HER2) overexpression is associated with aggressive tumors with increased incidence of metastasis and recurrence. Therapeutic antibodies such as Trastuzumab inhibit tumor growth through blockade of HER2 receptors. However, the short lifespan of such therapeutic antibodies necessitates repeat administrations with ensuing cardiac toxicity and development of resistance, while offering no protection against relapse. Cancer vaccines targeting HER2 can overcome these shortcomings of passive immunotherapy by instigating an endogenous and sustained immune response and memory against the cancer antigen. The efficacy of a viral nanoparticle (VNP)-based cancer vaccine is demonstrated here in activating a potent anti-HER2 immune response that delays progression of primary tumors as well as metastases and prolongs survival in mice. The results illustrate that the VNP-based vaccine instigates HER2-specific antibodies as well as effector and memory T cells, which contributes to the effectiveness of the vaccine. Given the highly aggressive course of $HER2^+$ cancers, inhibition of disease progression by such cancer vaccines could provide a critical window for interventions with other adjuvant therapies. Moreover, the immune memory generated by this viral nanoparticle-based cancer vaccine could mitigate relapse of the disease.

Keywords

cancer vaccine; HER2 breast cancer; lung metastasis; viral nanoparticle

1. Introduction

The human epidermal growth factor receptor 2 (HER2) is over-expressed in 20–30% of all breast carcinomas and is associated with aggressive tumors, high rates of metastasis and recurrence, and short disease free survival.[1] HER2 overexpression and its role in epithelial oncogenesis make it an attractive candidate for targeted therapies. Therapeutic antibodies such as Trastuzumab bind to the extracellular domain of HER2 receptor to block signaling and activate antibody-dependent cellular toxicity (ADCC),[2] while their derivatives such as Ado-Trastuzumab emtansine can deliver chemotherapy to cells with high specificity.[1b] On the other hand kinase inhibitors such as Laptinib function by binding to the catalytic

domains of HER2. These drugs are administered as mono or combination therapies along with conventional chemotherapy for maximal efficacy.[2]

While widely used in the clinic, HER2 targeting therapeutic antibodies are associated with cardiac toxicity and congestive heart failure, in particular their combination with chemotherapy regimens leads to significant untoward effects.[3] Limited patient sensitivity and development of early resistance to these monoclonal antibodies further limits the benefits of this approach. Moreover, passive immunotherapy does not protect against a relapse and given the short half-life of monoclonal antibodies, multiple administrations in large doses are required, that increases costs and requires frequent outpatient visits.[4] Active immunotherapy through cancer vaccines holds the potential to overcome these shortcomings through more effective, sustained immunity requiring fewer administrations, and offer long lasting immune memory against residual or returning cancer, thereby reducing costs, improving quality of life and most importantly patient survival.[5]

Several HER2 vaccine approaches including DNA-, whole protein- and peptide-based vaccines have been tested and are in different stages of development and clinical trials.[6] The primary objective here is to overcome the built-in tolerance for the HER2 self-antigen through an effective immune stimulus,[7] which requires efficient delivery of antigenic epitopes along with an adjuvant to the antigen presenting cells (APCs). Nanoparticles with their natural disposition to immune cells are excellent platforms to deliver large payloads of antigens and adjuvants.[8] Viral nanoparticles (VNPs) derived from plant viruses and bacteriophages are a class of biologics that has been shown to be particularly powerful platforms for vaccine applications.[9] With a polyvalent symmetry of the proteinaceous capsid, VNPs mimic the molecular patterns associated with pathogens, rendering them highly visible to the immune system. Therefore, the VNP is not simply a delivery agent, but itself functions as an adjuvant and stimulates the immune system for effective processing and presentation of the antigens leading to ensuing immune stimulation without requiring additional adjuvants.[10] Moreover, with well-defined structural knowledge and precision of chemical and genetic engineering methods, VNPs are ideal scaffolds for structure-based vaccine design and large-scale manufacturing.[11] In fact, plant-produced VLP-based influenza vaccine has completed a Phase 2 clinical trial[12] and a Phase 3 clinical trial is currently under way. We have previously compared and demonstrated that icosahedral VNPs display superior lymphatic drainage and immune cell interactions compared to filamentous, high aspect ratio plant VNPs.[13] The structure-function relationship study was focused on establishing the parameters influencing nanoparticle interactions with the components of the immune system.

In this work, we set out to evaluate the potency of Cowpea mosaic virus (CPMV) nanoparticle-based cancer vaccine in several mouse models of $HER2^+$ tumors in conjugation with the antigenic CH401 peptide derived from the extracellular domain of HER2 receptor.[14] We evaluated the vaccine efficacy in the settings of ectopic and orthotopic primary tumor challenge as well as with a metastatic tumor challenge using the aggressive DDHER2 cells in Balb/c mice.[15] We also evaluated the efficacy of the vaccine against a transplantable tumor derived from transgenic MMTV-neu mice that develop spontaneous $HER2^+$ tumors.[16] Furthermore, we evaluated the potential for synergy of the CPMV-HER2

vaccine when combined with an in situ vaccine strategy involving CPMV particles. Efficacy studies were paralleled with immunological studies to gain insights into the mechanism of the cancer vaccine.

2. Results and Discussion

We have previously demonstrated that individual VNPs have distinct advantages with icosahedral particles showing superior lymphatic drainage and immune cell interactions compared to filamentous, high aspect ratio plant VNPs.[13] We established the chemistry for formulating a plant virus-based HER2 vaccine candidate using the 30 nm-sized icosahedral nanoparticles from CPMV. Specifically, CPMV was engineered to display the HER2 epitope CH401, a potent epitope from the extracellular domain of HER2 containing an anchoring motif of MHC class II molecule. The CH401 peptide contains epitopes for both B-cells and helper T-cells.[14] In our previous work, we demonstrated that immunization of female FVB/N mice with this CPMV-CH401 vaccine led to high titers of HER2-reactive antibodies spanning the IgG1/2a/2b isotypes.[13]

With the chemistry of the CPMV-HER2 vaccine well established, in this work, we evaluated the anti-tumor activity of CPMV-CH401 vaccine in several mouse models of $HER2^+$ tumors to validate the potency of this vaccine candidate.

2.1. Synthesis and Immunogenicity of CPMV-CH401 Vaccine

All animal experiments were carried out in accordance with Case Western Reserve University's Institutional Animal Care and Use Committee. CPMV was propagated in and purified from black-eyed peas using established methods we reported previously.[17] The CPMV capsid is a 30 nm-sized icosahedron containing 60 copies each of a large (L, 42 kDa) and small (S, 24 kDa) coat protein arranged with pT = 3 icosahedral symmetry. The CH401 peptide, designed with=a flexible GPSL linker[18] and a C-terminal cysteine, was conjugated to CPMV via its solvent exposed Lys side chains[19] using a bi-functional N-hydroxysuccinimide-PEG4-maleimide (SM-PEG4) linker. The conjugation was as previously reported (Figure 1A). The resulting CPMV-CH401 particles remained structurally sound as determined by transmission electron microscopy (Figure 1B). Denaturing gel electrophoresis confirmed conjugation of CH401 to the CPMV coat protein (CP) as indicated by the appearance of additional higher molecular weight bands above the small CP (Figure 1C). The protein band intensity analysis indicated modification of nearly 50% of S-CP, which corresponds to ≈ 30 CH401 peptides per CPMV (Figure 1C). The modification of large coat protein is not clear enough for quantitative analysis.

The human HER2 protein erbB2 and the rat counterpart neu share 88% homology (UniProt P04626 and P06494, respectively). The 20-mer rat neu sequence homologue to the human $CH401_{163–182}$ domain differ in five amino acids ($human_{163–182}$: **YQDTILWKDIFHKNNQLALT**) versus $rat_{167–186}$: **YQDMVLWKDVFRKNNQLAPV**). Earlier studies have compared cross-reactivity of human HER2 and rat neu in vaccine formulations.[20] These results have indicated that in transplantable tumor models homologous vaccines are more efficient over heterologous vaccines.[20] On the contrary, in transgenic mouse models of HER2 tumors and in clinical studies, it has been demonstrated

homologous vaccines are unable to break self-tolerance of HER2.[7b,20–21] In this work we compared efficacy of CPMV-CH401 formulations with human (H) versus rat (R) versions of the CH401 epitope. Female Balb/c mice (n =10) were immunized subcutaneously with a 50 μg per injection=dose of CPMV-$CH401_H$ or CPMV-$CH401_R$ vaccines in PBS; the administration schedule (Figure 1D) was four biweekly treatments. Corresponding quantities of free peptides in PBS were also administered. Sera were collected from all mice prior to first immunization and then on each day of vaccination for analysis (Figure 1D). ELISAs performed on CH401-coated plates showed a steady increase in the CH401-specific IgG titers with successive immunizations; the titers peaked on day 28, indicating that a single booster dose is sufficient to generate a maximal titer (Figure 1E). As expected, CH401-specifc IgG titers from free peptide immunizations remained comparable to pre-immunization sera highlighting the need for an immunostimulatory carrier for delivery of the short peptides (Figure 1E). Between the formulations, immunization with CPMV-$CH401_R$ resulted in significantly stronger rat and human CH401-specific IgG response compared to CPMV-$CH401_H$ (Figure 1E and Figure S1, Supporting Information) with threefold higher peak titers (8100 versus 27 000 for CPMV-$CH401_{R\ versus}$ CPMV-$CH401_H$ tested against rat CH401; Figure 1E) suggesting stronger immunogenicity of the rat peptide in the mouse model. Next, IgG isotyping performed on recombinant rat HER2 protein coated plates revealed the presence of IgG1, IgG2a, and IgG2b isotypes in mouse sera from both the rat and human CH401 vaccine formulations (Figure 1F). Both vaccine formulations stimulated comparable levels of IgG1 and IgG2a isotypes and significantly higher levels of IgG2b (Figure 1F). Thus, the CPMV-based vaccines produced a broad spectrum of IgG isotypes including high IgG2a/2b titers that are critical for effector functions through the Fc receptors.

Our previous study in FVB mice has looked into the mechanistic aspects of plant VNP derived cancer vaccines. We have illustrated that the enhanced immunogenicity observed for HER2 derived peptide epitopes presented on the particulate CPMV carrier arise from efficient antigen delivery. We and others have showed that the lymphatic drainage and or nanoparticulate carriers and adjuvants is dependent on particle size and geometry.[8c,10a,13] The 30 nm CPMV icosahedron showed efficient trafficking to and retention within the draining lymph nodes (dLNs) following sub-cutaneous injections, where they are taken up by APCs including dendritic cells (DCs) and macrophages. We further illustrated that CPMV VNPs resulted in activation of DCs and macrophages as indicated by significantly increased CD86 and CD40 expression.[13] Our current results corroborate previously observed behavior of CPMV and confirmed the immunogenicity of CPMV-$CH401_R$ vaccine in our experimental mouse model.

Next, we evaluated the ability of the mouse sera to recognize and bind cellular HER2 receptor on DDHER2 cells using confocal microscopy and flow cytometry (Figure 1G,H). Confocal results show that both CPMV-$CH401_R$ sera and CPMV-$CH401_H$ sera recognize and bind to cellular HER2 receptors on DDHER2 cells (Figure 1G). However, quantitative analysis using flow cytometry suggests that the former showed significantly higher binding over the latter (Figure 1H). This is as expected because the DDHER2 cells express rat neu and highlights the need for species-specific formulations when developing and testing vaccines.

Following this, we evaluated the ability of CH401-specific antisera to neutralize HER2 expressing cancer cells using a MTT assay. We compared the CPMV-$CH401_R$ sera and $CH401_R$ sera with naïve sera from nonimmunized mice and with an anti-HER2 IgG to determine complement dependent cytotoxicity (CDC) against DDHER2 cells (Figure 1I). We observed that under the tested conditions, sera from CPMV-CH401 or CH401 immunized mice showed significantly stronger cytotoxicity over naïve sera. Thus, CH401-specific IgGs are able to recognize and bind to the cellular HER2 proteins and lead to complement mediated cytotoxicity similar to the effects exerted by the commercial anti-HER2 IgGs. While the CPMV-CH401 sera exerted elevated cytotoxicity over CH401 sera, the differences were not statistically significant under the tested in vitro conditions (low DDHER2 cell numbers and high sera concentrations) despite a significant difference in the anti-CH401 IgG titers between the two groups (Figure 1E). To validate our results depicting enhanced immunogenicity of CPMV-CH401 vaccine, we next compared the vaccine efficacy in vivo.

2.2. Testing Vaccine Efficacy in Primary and Metastatic Tumor Settings

Cancer vaccines have been generally classified as therapeutic vaccines and considered as adjuvant therapies post-surgical resection of the primary tumor. An effective cancer vaccine should be able to generate tumor antigen-specific cellular and/or humoral responses capable of recognizing residual or recurring cancer.[22] With an anti-HER2 antibody response from the CPMV-based vaccines validated, we first compared the anti-tumor activity of the rat neu and human erbB2-specific vaccines in an orthotopic model using DDHER2 cells and Balb/c mice. Female Balb/c mice were immunized twice on day 0 and 14 with 50 μg of CPMV-$CH401_{R/H}$ or 2 μg of corresponding free peptides (the free peptide dose was normalized to the CPMV-$CH401_{R/H}$ dose). On day 19 after the first immunization, mice were challenged with an orthotopic inoculation of 2×10^6 DDHER2 cells in the inguinal mammary fat pads. Subsequently, two more doses of vaccines were administered 10 and 27 days following the tumor challenge (Figure 2A). Control mice were challenged with tumors similarly but only received subcutaneous PBS injections as a mock immunization (Figure 2A). Tumor growth was monitored daily once palpable tumors were observed.

Compared to control mice, CPMV-$CH401_R$ and CPMV-$CH401_H$ vaccine immunized mice showed significantly slower tumor growth over 52 days of monitoring (Figure 2B,C). It should be noted here that the tumor growth in immunized mice was impeded but never regressed. However, at day 52, the mean tumor volume of the PBS group was 1099 mm^3, while the CPMV-$CH401_R$ and CPMV-$CH401_H$ mean volumes were 448 mm^3 and 660 mm^3, respectively. Also, throughout this period, the free peptide vaccine was outperformed by the CPMV-based vaccine from both groups and a larger proportion of CPMV-vaccine immunized mice demonstrated tumor volumes below 500 mm^3 compared to peptide-immunized mice on day 54 from tumor challenge (Figure S2, Supporting Information). These results clearly underline the effectiveness of CPMV-CH401 vaccine in delaying orthotropic DDHER2 tumor growth. Our results also suggested that both rat and human vaccine formulations effectively slowed down the tumor growth. However, differences in the mean tumor volumes over the course of study could be correlated to the higher immunogenicity of the rat peptide as indicated by the elevated IgG titers from the CPMV-

$CH401_R$ vaccine (Figure 1). These results also corroborate previous studies suggesting higher efficacy of homologous vaccines in transplantable tumor models. Based on this, we used the CPMV-$CH401_R$ vaccine for all our subsequent experiments.

To further assess how robust the cancer vaccine is, we evaluated its efficacy in two additional settings using the DDHER2 cells: First, we evaluated the vaccine efficacy in a subcutaneous DDHER2 tumor model that showed a more aggressive growth pattern over the orthotopic model. Female Balb/c mice were immunized six times bi-weekly with CPMV-$CH401_R$ vaccine with two vaccinations occurring prior to tumor challenge, that is, the vaccine was given on 28 and 14 days prior to tumor challenge and bi-weekly vaccinations continued through day 42 post tumor challenge. The treatment group receiving the vaccine candidate CPMV-$CH401_R$ was compared with groups receiving free $CH401_R$ peptide or PBS (Figure 2D). Tumors in PBS and free peptide groups grew rapidly and reached endpoint volumes around 30 days from inoculation, suggesting free peptide immunization without an adjuvant offers no protection against an aggressive $HER2^+$ cancer. In stark contrast, mice immunized with CPMV-$CH401_R$ showed a significantly delayed tumor progression over a 50-day period (Figure 2E), resulting in an overall survival advantage of 3 weeks over nonimmunized mice (Figure 2F).

Metastasis is the main cause of mortality in breast cancer. $HER2^+$ breast cancer in particular has an enhanced tendency to metastasize to distant organs including lungs, liver, bones, and brain.[1b,23] While primary tumors are subject to aggressive treatment regimens, metastases detection generally corresponds to an advanced stage of tumor, where the overall therapeutic goal is to prolong survival and generally, aggressive treatment is not pursued.[24] To determine if HER2-reactive IgGs in sera could prevent lung metastasis, we challenged groups of control ($n = 3$), CPMV-$CH401_R$ ($n = 5$) or free $CH401_R$ immunized mice ($n = 5$) with intravenous injections of bioluminescent DDHER2 cells (DDHER2-luc) obtained by transfecting DDHER2 cells with firefly luciferase using method described previously (Supporting Information)[25] (Figure 2G). Intravenously administered cancer cells rapidly home to lungs; disease burden in the lungs was monitored using bioluminescence imaging (Figure 2H,I). Control mice started showing metastatic lesions in lungs as early as 6 days following the tumor challenge, and had significantly higher signal intensities over immunized mice. By day 12, intense bioluminescence signals were observed in all three PBS treated control mice; the mice showed clear signs of respiratory stress and were euthanized. Similarly, metastatic lesions were observed in CH401 peptide immunized mice starting on day 9; however, disease burden in four of these mice significantly increased and was comparable to the control mice by day 12 (Figure 2I). In stark contrast, mice from the CPMV-CH401 treatment arm showed negligible bioluminescence signals that remained significantly lower than both control and CH401 groups up to day 12 (Figure 2I). These results corroborate our observations from the orthotropic and subcutaneous tumor studies. Even the CPMV-CH401 immunized mice eventually developed lung metastases; however survival was prolonged for several days as mice were euthanized after day 16 (as opposed to day 12 for the PBS and free peptide control groups).

In a further set of studies, we evaluated the vaccine efficacy in immunized FVB/N mice that were challenged with orthotropic implants of $HER2^+$ tumors derived from the transgenic

MMTV-neuT strains. Female transgenic MMTV-neuT mice express neu under the transcriptional control of the mouse mammary tumor virus promoter.[16] The females of this transgenic strain develop spontaneous tumors by 25–29 weeks of age. Tumors derived from transgenic females were collected and cut into small pieces of 2.5–3 mm; these were then surgically transplanted into the mammary fat pads of female FVB/N mice immunized with CPMV-CH401 vaccine, CH401 peptide, or PBS ($n = 9$) (Figure 3A). Tumor growth arising from cancerous tissues in this model was slower and showed more variation due to heterogeneity of tumor pieces. However, consistent with the aforementioned studies, tumor burden was reduced in CPMV-CH401 vaccinated animals. While non-vaccinated control mice (receiving PBS treatments) reached endpoint tumor volumes in 50–55 days post tumor implantation, immunized mice receiving CPMV-CH401 or free CH401 peptide showed distinct populations of responders versus nonresponders where ≈ 55% of mice showed noticeably slower tumor growth as compared to nonimmunized mice (Figure 3B). Amongst this population of responders, however, there was nearly twofold difference in the tumor volumes of CPMV-CH401 immunized and free peptide administered mice (mean tumor volumes CPMV-CH401 responders versus CH401 responders for n ≥ 3: 85.05 mm^3 versus 253.5 mm^3 (day 45), 151.6 mm^3 versus 372.6 mm^3 (day 49), 191.1 mm^3 versus 464.2 mm^3 (day 52), and 409.4 mm^3 versus 1002.43 mm^3 (day 58)). Overall, immunized mice showed a survival benefit of nearly 40 days compared to nonimmunized mice (Figure 3B). We selected CH401 as epitope of choice based on its immunogenicity as reported earlier. It is apparent that in slow growing tumors, such as the orthotropic models discussed above, the peptide vaccine does show partial response in terms of slower tumor growth as compared to nonimmunized mice. In conjugation with the CPMV carrier, however a more pronounced effect is obtained. A clearer and significant difference in the efficacy of VNP vaccine and free peptide is seen in the aggressively growing subcutaneous tumors, where CPMV-CH401 vaccine delayed tumor growth and enhanced survival.

Together, this set of studies demonstrates that the CPMV-CH401 vaccine candidate can effectively overcome the tolerance against the self-antigen and stimulate a strong humoral response capable of recognizing HER2 expressing tumor cells and slowing down growth of primary tumor as well as prevent metastatic spread.

To gain an insight into the mechanism of the CPMV-CH401-induced anti-tumor immunity, we isolated splenocytes from immunized Balb/c mice following three immunizations and compared T cell populations following ex vivo stimulation with the CH401 peptide via intracellular IFN-γ staining (Figure 4A). Cells were pre-gated with CD3 marker to distinguish $CD4^+$ and $CD8^+$ T cells subsets; subsequently CD4 and CD8 pre-gated cells were gated for CD44 to determine the fraction of effector:memory cell populations. We observed a significant increase in both IFN-γ^+ $CD4^+$ T cells and IFN-γ^+ $CD8^+$ T cells in the CPMV-CH401 vaccine group over peptide immunized and nonimmunized groups (Figure 4B,C). While $CD8^+$ T cells are the main players in the cytotoxic T cells (CTL) response, $CD4^+$ T cells are critical for initiating and maintaining the CTL response against tumors.[26] $CD4^+$ T helper cells activate APCs[27] and enhance expression of MHC and co-stimulatory molecules such as IL-12 that are crucial for an effective CTL response. $CD4^+$ T helper cells also secrete IL-2 that recruits CTLs to tumor sites.[28] IFN-γ production by $CD4^+$ T helper cells also upregulate the expression of MHC molecules on tumor cells leading to enhanced

CTL recognition. In addition to supporting the primary CTL activity, $CD4^+$ T helper cells also play a role in generating and maintaining memory $CD8^+$ T cells.[29] Effective priming of $CD4^+$ and $CD8^+$ T cells is thus an important goal and was achieved using the CPMV-CH401 vaccine candidate with contributing effects from both carrier and epitope. The CH401 peptide has been reported to consist of both B-cell and T-helper cell epitopes[14] while VNPs with their intrinsic immunogenicity serve as adjuvants and are considered activators of $CD4^+$ T helper cell response.[30] In addition, our results showed that the immunized group also boasted elevated fractions of IFN-γ^+ $CD4^+$ $CD44^+$ and $CD8^+$ $CD44^+$ effector memory cells (Figure 4B,C), indicating the vaccine candidate primes durable anti-tumor immunity. Earlier studies have suggested that suppression of anti-HER2 Th1 response could promote tumorigenesis[31] and is correlated with lack of response to neoadjuvant therapies. On the other hand, vaccines bearing potent $CD4^+$ T helper epitopes have been shown to generate a more efficient CTL response against large doses of tumor cell challenges.[32] Therefore, in addition to arresting tumor progression, a HER2 vaccine such as CPMV-CH401 could facilitate effectiveness of other anti-HER2 therapies by enhancing HER2-specific Th1 response.

Lastly, we tested the efficacy of combination immunotherapies. As noted earlier, while we noted significant delay in tumor and metastatic outgrowth upon vaccination with the CPMV-CH401 vaccine, disease elimination was not achieved. This highlights the aggressive nature of the DDHER2 tumor model, and also reflects on the poor prognoses in patients with $HER2^+$ malignancies. Combinatorial approaches hold promise to boost the efficacy of cancer vaccines.[15,33] Tumor antigen-specific antibodies, such as those generated by cancer vaccines can recognize and bind to transformed cells, but rely on the engagement of Fc-receptor expressing effector cells to kill the tumor cells through specific mechanisms including ADCC and phago-cytosis. Stimulation of such effector cells could therefore enhance the therapeutic efficacy of the antibodies and vaccines. Several such approaches involving immunomodulators and cytokines are currently being evaluated to activate NK cells, dendritic cells, and macrophages.[34] We hypothesized that the combination of the HER2 vaccine with an immunotherapy approach that attracts immune cells into the tumor bed may improve the efficacy of the vaccine. Toward this end, we and others have recently demonstrated the potential of plant VNP-based in situ vaccination.[35] Here the immunostimulatory agent, the VNP, is administered directly into an identified tumor to modulate the local tumor microenvironment from immune-suppressive to immune-supportive, resulting in infiltration and activation of a broad spectrum of immune effector cells leading to local and systemic anti-tumor immune response.[35] We therefore reasoned that combining the CPMV-HER2 vaccine with the in situ vaccination approach (intratumoral administration of CPMV) could enhance the potency of the tumor antigen specific antibodies by the enriched milieu of effector cells in the tumor microenvironment. To test this hypothesis, female Balb/c mice received two immunizations with the CPMV-CH401 vaccine candidate; following tumor challenge with subcutaneous DDHER2 tumors in the flank, an additional two vaccinations were given (Figure 5A). Starting at day 15 post-tumor inoculation, that is, when tumors were established, in situ vaccination was initiated and CPMV (100 μg of CPMV in 20 μL PBS per each tumor) was administered by intratumoral (I.T.) injections on a weekly basis for 4 weeks. Tumor growth was measured and results

were compared with control mice (nonimmunized, no I.T. CPMV), CPMV vaccine PBS I.T. group, PBS S.C. + CPMV I.T., and CPMV-CH401 vaccine + S.C. + CPMV I.T. groups. Our results indicated that mice receiving intratumoral CPMV injections alone or CPMV-CH401 vaccine alone showed comparably inhibited tumor growth patterns (Figure 5B), with a survival period of 44 days as compared to the rapid growth of untreated tumors with an overall survival of 28 days (Figure 5C). Most importantly, the combination of these two approaches leads to a greater survival benefit than either single agent. Mice from the combination treatment arm showed a significantly slower tumor growth with average tumor volumes that were half of control mice by day 30 and an overall survival of 56 days. (Figure 5C).

Together, these results illustrate that plant VNPs with their inherent immunostimulatory nature are excellent carriers of tumor antigens and can lead to a strong and sustained anti-tumor immune response. These biocompatible carriers obviate the need for additional adjuvants. With the possibility of genetic engineering, future designs could incorporate the tumor antigens into the viral coat proteins, thus providing a means of cost-effective manufacture without batch-to-batch variations. Our data also indicate that combination immunotherapy with in situ vaccines and epitope display strategies may be beneficial in settings where patients have highly aggressive primary tumors. Alternate combinations with targeted chemotherapy and/ or immunotherapies such as checkpoint blockade could also result in a more conducive tumor microenvironment for the effector functions to take place. Furthermore, there is room for further engineering; for example, the CPMV-based HER2 vaccine could be further enhanced by incorporating multiple B- or T-cell epitopes to broaden the immune response and repertoire of antibodies thereby preventing immune-evasion by mechanisms such as immune-editing and antigen shedding. In conclusion our studies validate the potency and potential of CPMV-based cancer vaccines.

3. Conclusions

The relapse and metastatic spread of $HER2^+$ breast cancers remains the primary cause of mortality in patients following surgical intervention. Disease management using adjuvant therapies based on humanized anti-HER2 monoclonal antibodies is hampered by development of resistance and toxicity associated with repeated dosing. Cancer vaccines targeting HER2 are promising alternatives that offer an active and durable immunity against the antigen. However, the potency of such a vaccine relies on efficient delivery of tumor antigens to APCs along with the immunostimulatory impetus of a potent adjuvant.

In this study, we have demonstrated the potency of plant viral nanoparticle CPMV-based HER2 vaccine to induce a strong and sustained anti-HER2 immune response. The efficacy of this vaccine to regress tumor growth and prolong survival is then illustrated using primary and metastatic mice models of $HER2^+$ cancer. Given the simplicity of design and manufacturing, such therapeutic vaccines based on the biocompatible CPMV platform technology could offer cost effective and potent alternatives to current adjuvant therapies.

4. Experimental Section

VNP Propagation:

Established procedures were used for the propagation and purification of CPMV.[17] Purified VNPs were stored in potassium phosphate buffer (0.1 m, pH 7.0) at 4 °C. Concentrations of VNPs were determined by UV spectroscopy at 260 nm using the molar extinction coefficients $\varepsilon_{CPMV} = 8.1$ mL mg^{-1} cm^{-1}.

Synthesis of the CPMV Vaccine Formulation:

Human HER2 epitope CH401and the rat analogue with GPSL linker and terminal Cysteine residue were procured from Genscript: $Human_{163–182}$: YQDTILWKDIFH-KNNQLALT-GPSL-C versus $Rat_{167–186}$: YQDMVLWKDVFRKNNQLAPV-GPSL-C. In a two-step protocol, cysteine-terminated peptide epitopes with flexible GPSL linker[18,36] were conjugated to VNPs via the heterobifunctional *N*-hydroxysuccinimide-PEG_4-maleimide linker SM-PEG4 (Life Technologies). Briefly, CPMV was reacted with 3500 molar excess of SM-PEG4 linker at room temperature for 2 h at a 2 mg mL^{-1} CPMV concentration followed by a 5000 molar excess of peptides overnight. CPMV-CH401 formulations were purified over a 40% w/v sucrose cushion at 160 000 × *g* for 3 h and resuspended in sterile PBS.

Vaccine Characterization:

To verify peptide conjugation, unmodified CPMV, CPMV-SM(PEG)4 intermediate, and purified CPMV-CH401 (20 μg of each) were compared by SDS electrophoresis using pre-cast NuPAGE 4–12% Bis-Tris proteins gels (ThermoFisher Scientific). AlphaImage gel documentation system (Protein simple) was used to capture image of gel stained with GelCode Blue Safe protein stain (ThermoFisher Scientific) and lane density analysis (ImageJ 1.44o software, http://imagej.nih.gov/ij) was used to quantify peptide conjugation. Particle integrity was confirmed by transmission electron microscopy (TEM) using FEI Tecnai F30 instrument following uranyl acetate staining.

Immunizations:

All animal experiments were carried out in accordance with Case Western Reserve University's Institutional Animal Care and Use Committee. 7–8 week old female Balb/c mice (Charles River, NJ) or FVB/N mice (Jackson lab) were immunized with 50 μg CPMV-CH401 vaccine or CH401 peptide (2 μg) in PBS (100 μL) through subcutaneous injections. Blood was collected through retro-orbital bleeding and centrifuged at 14 800 rpm for 10 min to separate the serum, which was then stored at 4 °C until analyzed.

Antibody Titers and Isotypes:

ELISAs were carried out to determine levels of CH401 peptide specific IgG titers and HER2 specific IgG isotypes. Peptide-specific IgG ELISA was performed on the 96-well Pierce Maleimide Activated Plates (Thermo Fisher Scientific) prepared and processed as per manufacturer's instructions and coated with CH401 peptide (1 μg per well). Sera from immunized mice at various dilutions were incubated in the wells at 37 °C for 2 h. Plates

were washed four times with washing buffer (0.05% v/v Tween-20 in PBS, 200 μL per well) between all steps. Plates were then incubated with 100 μL of alkaline phosphatase-labeled goat anti-mouse IgG (Invitrogen, Thermo Fisher Scientific) in blocking buffer (at 1:3000 dilution) at 37 °C for 1 h and developed with 100 μL of 1-step PNPP substrate (Thermo Fisher Scientific) for 10 min at 4 °C. Reaction was stopped using 2 M NaOH (50 μL). Absorbance was then read at 405 nm using a Tecan microplate reader. IgG isotyping was similarly performed against HER2 protein using Ni-activated plates coated according to manufacturers' instructions with 1 μg recombinant rat or human HER2/ ErbB2 protein containing His-tag (Acro Biosystems, Newark, DE).

Cell Lines:

DDHER2 cell line was a gift from Dr. Darrel Irvine's lab at MIT, Cambridge-MA. Cells were maintained on DMEM media containing 25 mm HEPES and supplemented with 10% v/v fetal bovine serum and 1% v/v Penicillin/Streptomycin (all reagents from Life Technologies, Grand Island, NY) at 37 °C and 5% CO_2. DDHER2-Luc cell line used for in vivo tracking was generated by stably transfecting DDHER2 cells using transformation protocol described previously.[25]

Cell Binding Assay:

For confocal studies, 25 000 DDHER2 cells per well were cultured on glass coverslips in a 24-well suspension culture plate for 24 h. Pooled antisera from immunized mice were added with fresh culture media (1:100 dilution) and incubated with cells at 4 °C for 2 h. Post-incubation, cells were washed, fixed, and stained with goat anti-mouse-AlexaFluor 488 secondary antibody (1:1000 dilution; Life Technologies). Confocal images were captured on an Olympus Flu-oViewTM FV1000 LSCM and data processed using ImageJ 1.44o software (http://imagej.nih.gov/ij). Cell binding was quantified using flow cytometry. DDHER2 cells were collected in enzyme-free Hank's-based Cell Dissociation Buffer (Fisher), and resuspended in 200 μL of complete medium in a 96-well plate at 200 000 cells per well, then incubated for 2 h at 4 °C with sera from naïve and immunized mice (1:100 dilutions). Post-incubation, cells were washed twice in FACS buffer (1 mm EDTA, 25 mm HEPES, 1% v/v FBS in PBS, pH 7.0), fixed in 2% v/v paraformaldehyde and washed twice again, then stained with goat anti-mouse IgG antibody conjugated with AlexaFluor 488 (1: 1000 dilution) for 60 min at 4 °C. BD LSR II Flow Cytometer was used for cytometry and FlowJo v8.6.3 software used for analyses.

Complement-Dependent Cytotoxicity:

DDHER2 cells re-suspended in 200 μL FACS buffer in a 1.5-mL Eppendorf tube (at 80 000 cells per tube) were incubated for 1 h at 4 °C with mouse serum diluted 1:50 with FACS buffer or similar dilutions of rabbit polyclonal anti-HER2 Ab (Novus Biologicals). After three times washing with PBS, the cells were re-suspended in 200 μL serum-free medium and transferred to 96-well plates in four replicates (20 000 cells per well in 50 μL medium). Rabbit C12CC complement (BioRad) was diluted 1:20 in serum-free medium and added to the plate (50 μL per well). Rabbit complement inactivated by heating at 65 °C for 30 min was incubated with cells that had not been exposed to mouse serum as a control representing 100% cell viability. Cells were incubated at 37 °C with 5% CO_2 for 4 h before adding 100

μL per well of 0.5% methylthiazolyldiphenyl-tetrazolium bromide (MTT) in PBS. After incubation at 37 °C for 2 h, the solution was carefully removed and 100 μL per well of DMSO was added before measuring the absorbance at 490 nm on a Tecan microplate reader.

Vaccine Efficacy Studies:

Female Balb/c mice were challenged with 2×10^6 DDHER2 cells in 50 μL sterile PBS under anesthesia using a Hamilton needle in the mammary fat pad. Sutures were applied to close the wound and mice were administered with Carpofen (5 mg kg^{-1}) subcutaneously for 3 days post surgery and observed for any discomfort for 72 h. Mice were monitored for appearance of palpable tumors and later tumors were measured using digital calipers. Tumor volumes were calculated as 0.5*(length × $width^2$); a 1000 mm^3 volume was considered end point volume and mice were euthanized thereafter. For subcutaneous tumors, 2×10^6 DDHER2 cells (in 100 μL of DMEM + Matrigel) were inoculated under the skin on right flank using a 26-gauge needle. Tumors were monitored as above. For metastatic studies, 1×10^6 DDHER2 cells in 200 μL of sterile PBS with 0.3% FBS were injected intravenously through tail vein. Tumors were monitored using bioluminescence imaging. Mice were injected intraperitoneally with luciferin (15 mg mL^{-1}, 150 μL) and imaged 5 min post-injection using a PerkinElmer IVIS Spectrum in vivo imaging system. For FVB/N studies, tumors derived from transgenic FVB/N (MMTVneu) mice were cut into 2.5–3 mm pieces and were surgically implanted into mammary fat pad. Following surgery, similar precautions were taken as above and tumors were monitored similarly. For in situ vaccination, subcutaneous tumors were injected with 100 μg of CPMV in 20 μL of sterile PBS using a 30 gauge, 0.5 inch needle. The needle was retracted slowly to avoid any solution loss. Detailed dosing information and administration scheduled are provided in the main text of the manuscript.

Splenocyte Isolation, Ex Vivo Stimulation, and Flow Cytometry:

Immunized and nonimmunized mice ($n = 5$) were euthanized 7 days after last vaccination and spleens were harvested under aseptic conditions in ice cold RPMI media. Single cell suspension was obtained by passing the spleens through 40 μm cell restrainer. Cells were then rinsed and spun at 200 g for 5 min, supernatant was discarded and pellet resuspended in 5 mL of RBC lysis buffer on ice for 5 min. Reaction was stopped by diluting the lysis buffer. Cells were centrifuged and re-suspended in RPMI media and counted. Splenocytes (10^6 cells per mL) were re-stimulated with 20 μg of CH401 peptide for 24 h at 37 °C. For the last 5 h brefeldin A (10 mg mL^{-1}) was added into the medium. Cells were then washed in PBS and resuspended in staining buffer (PBS 2% FBS, 0.1% sodium azide). Surface staining was performed for 30 min at 4 °C in dark with the following fluorescently labeled antibodies: Pacific blue-CD45 (30-F11), APC/Cy7-CD3ε (145–2V11 A); FITC-CD4 (GK1.5), APC-CD8α (53–6.7), PE-CD44 (IM7), and isotype controls (Biolegend). Then, cells were fixed in 3% paraformaldehyde, permeabilized with 0.1% saponin, then incubated with PE/Cy7-anti-IFN-γ (XMG1.2) Ab (BioLegend) for 30 min in 0.1% saponin. Cells were washed twice and resuspended in staining buffer before acquisition. Flow cytometry analyses were performed on a BD LSRII cytometer (BD Biosciences), and data were analyzed using the FlowJo software. OneComp eBeads (eBiosciences) were used as compensation controls.

Statistical Analysis:

All statistical analyses were performed using the GraphPad Prism 7 software. For immunogenicity studies (Figure 1), following groups were compared: CPMV-CH401H (n = 9), CPMV-CH401R (n = 10), CH401H (n = 10), CH401R (n 10). All ELISAs were performed using pooled sera from treatment groups=in three replicates/ sample. Data are plotted as mean with SEM. Statistical significance between the groups were compared by 2way ANOVA using Tukey's multiple comparisons test and p-values have been reported (****p < 0.0001, ***p < 0.001, **p < 0.01, *p < 0.05 and ns no significance). Flow cytometry experiments were performed on cells in three replicates/ sample, data analyzed using ordinary one-way ANOVA (****p < 0.0001). Cytotoxicity analyses was performed in four replicates/ sample, data analyzed with ordinary one-way ANOVA (****p < 0.0001; ***p < 0.001). For in vivo vaccine efficacy using orthotropic model in Balb/c mice (Figure 2A–C), mice were immunized with CPMV-CH401$_R$ (n = 10) and CPMV-CH401$_H$ vaccines (n = 9) or free peptides (n = 10) or PBS (n = 10). Data is plotted as mean with SEM to day where $n \geq 5$ for each group. Statistical analysis between tumor volumes on days 20, 30, 40, and 55 was performed using ordinary one-way ANOVA using Tukey's multiple comparison (**p < 0.01, *p < 0.05). For subcutaneous tumor studies (Figure 2D–F), n = 10 was used for all three groups. Data is plotted to day where $n \geq 5$ for each group. Statistical analysis between tumor volumes on days 30 was performed using ordinary one-way ANOVA using Tukey's multiple comparison (****p < 0.0001, **p < 0.01). Overall survival benefits between the immunized and control group was compared using Kaplan–Meier plot. Statistical analysis on the survival curves was performed using Log-rank (Mantel–Cox) test (***p < 0.001, *p < 0.05). For lung metastases study PBS (n = 3), CPMV-CH401 vaccine (n = 5) and CH401 (n = 5) were signal compared. Bioluminescence intensities were compared using ROI analysis (total counts) performed with the Living Image Software (PerkinElmer). Statistical analysis between treatment groups was performed using two-way ANOVA using Tukey's multiple comparison test (***p < 0.001, *p < 0.05). For transplant tumor studies (Figure 3), n = 10 female FVB mice were used for all groups. Tumor growth monitoring data is plotted as scatter dot plot with mean and SD. Kaplan–Meier plot have been used to compare the survival benefits offered by the vaccine over control mice. Statistical analysis on the survival curves was performed using Log-rank (Mantel–Cox) test (**p < 0.01). For splenocyte analyses using flow cytometry (Figure 4) n = 5 mice per group used. Ex vivo stimulation and staining for flow cytometry was performed in triplicates. Cytometry data were analyzed using the FlowJo software. Data is plotted as averages and SD; statistical analysis was performed by one-way ANOVA using Tukey's multiple comparison test with, **p < 0.005, *p < 0.05. For combination therapy (Figure 5) n = 10 was used for all groups except PBS s.c/ PBS i.t. (n = 8). Tumor volumes were plotted to days where n ≥ 5. Statistical analysis was performed by ordinary one-way ANOVA using Tukey's multiple comparison tests (****p < 0.0001, **p < 0.001, *p < 0.01). C) Kaplan–Meier plot compared the survival benefits; statistical analysis on the survival curves was performed using Log-rank (Mantel–Cox) test (****p < 0.0001; ***p < 0.001, *p < 0.05).

Supplementary Material

Refer to Web version on PubMed Central for supplementary material.

Acknowledgements

This work was partially supported by a grant from the Susan G. Komen foundation (CCR14298962 to N.F.S.) and NCI-Nanotechnology Alliance Grant (U01CA218292 to N.F.S.). DDHER2 cells were kindly provided by Prof. Darrel Irvine from MIT.

References

[1]. a)Wolff AC, Hammond ME, Hicks DG, Dowsett M, Mc-Shane LM, Allison KH, Allred DC, Bartlett JM, Bilous M, Fitzgibbons P, Hanna W, Jenkins RB, Mangu PB, Paik S, Perez EA, Press MF, Spears PA, Vance GH, Viale G, Hayes DF, American Society of Clinical Oncology, College of American Pathologists, J. Clin. Oncol 2013, 31, 3997; [PubMed: 24101045] b)Loibl S, Gianni L, Lancet 2017, 389, 2415. [PubMed: 27939064]

[2]. Gianni L, Eiermann W, Semiglazov V, Manikhas A, Lluch A, Tjulandin S, Zambetti M, Vazquez F, Byakhow M, Lichinitser M, Climent MA, Ciruelos E, Ojeda B, Mansutti M, Bozhok A, Baronio R, Feyereislova A, Barton C, Valagussa P, Baselga J, Lancet 2010, 375, 377. [PubMed: 20113825]

[3]. Florido R, Smith KL, Cuomo KK, Russell SD, Am J. Heart Assoc. 2017, 6, e006915.

[4]. a)Garrison LP Jr.,Lubeck D, Lalla D, Paton V, Dueck A, Perez EA Cancer 2007, 110, 489; [PubMed: 17592827] b)Guerin A, Lalla D, Gauthier G, Styles A, Wu EQ, Masaquel A, Brammer MG, SpringerPlus 2014, 3, 236. [PubMed: 24936383]

[5]. Ladjemi MZ, Jacot W, Chardes T, Pelegrin A, Navarro-Teulon I, Cancer Immunol., Immunother. 2010, 59, 1295.

[6]. Baxevanis CN, Voutsas IF, Gritzapis AD, Perez SA, Papamichail M, Immunother. 2010, 2, 213.

[7]. a)Bright RK, Bright JD, Byrne JA, Hum. Vaccines Immunother. 2014, 10, 3297;b)Disis ML, Shiota FM, Cheever MA, Immunology 1998, 93, 192. [PubMed: 9616368]

[8]. a)Pilla L, Rivoltini L, Patuzzo R, Marrari A, Valdagni R, Parmiani G, Expert Opin. Biol. Ther 2009, 9, 1043; [PubMed: 19591629] b)Fang RH, Kroll AV, Zhang L, Small 2015, 11, 5483; [PubMed: 26331993] c)Manolova V, Flace A, Bauer M, Schwarz K, Saudan P, Bachmann MF, Eur. J. Immunol 2008, 38, 1404; [PubMed: 18389478] d)Fan Y, Kuai R, Xu Y, Ochyl LJ, Irvine DJ, Moon JJ, Nano Lett. 2017, 17, 7387. [PubMed: 29144754]

[9]. a)Jobsri J, Allen A, Rajagopal D, Shipton M, Kanyuka K, Lomonossoff GP, Ottensmeier C, Diebold SS, Stevenson FK, Savelyeva N, PLoS One 2015, 10, e0118096; [PubMed: 25692288] b)Plummer EM, Manchester M, Wiley Interdiscip. Rev. Nanomed. Nanobiotechnol 2011, 3, 174;c)Noad R, Roy P, Trends Microbiol. 2003, 11, 438; [PubMed: 13678860] d)Scheerlinck JP, Greenwood DL, Drug Discovery Today 2008, 13, 882. [PubMed: 18656548]

[10]. a)Bachmann MF, Jennings GT, Nat. Rev. Immunol 2010, 10, 787; [PubMed: 20948547] b)Lee KL, Twyman RM, Fiering S, Steinmetz NF, Wiley Interdiscip. Rev. Nanomed. Nanobiotechnol 2016, 8, 554.

[11]. Landry N, Pillet S, Favre D, Poulin JF, Trepanier S, Yassine-Diab B, Ward BJ, Clin. Immunol 2014, 154, 164. [PubMed: 25128897]

[12]. a)Pillet S, Aubin E, Trepanier S, Bussiere D, Dargis M, Poulin JF, Yassine-Diab B, Ward BJ, Landry N, Clin. Immunol 2016, 168, 72; [PubMed: 26987887] b)Pillet S, Aubin E, Trepanier S, Poulin JF, Yassine-Diab B, Meulen J. Ter, Ward BJ, Landry N, npj Vaccines 2018, 3, 3. [PubMed: 29387473]

[13]. Shukla S, Myers JT, Woods SE, Gong X, Czapar AE, Commandeur U, Huang AY, Levine AD, Steinmetz NF, Biomaterials 2017, 121, 15. [PubMed: 28063980]

[14]. Miyako H, Kametani Y, Katano I, Ito R, Tsuda B, Furukawa A, Saito Y, Ishikawa D, Ogino K, Sasaki S, Imai K, Habu S, Makuuchi H, Tokuda Y, Anticancer Res. 2011, 31, 3361. [PubMed: 21965747]

[15]. Moynihan KD, Opel CF, Szeto GL, Tzeng A, Zhu EF, Engreitz JM, Williams RT, Rakhra K, Zhang MH, Rothschilds AM, Kumari S, Kelly RL, Kwan BH, Abraham W, Hu K, Mehta NK, Kauke MJ, Suh H, Cochran JR, Lauffenburger DA, Wittrup KD, Irvine DJ, Nat. Med 2016, 22, 1402. [PubMed: 27775706]

[16]. Guy CT, Webster MA, Schaller M, Parsons TJ, Cardiff RD, Muller WJ, Proc. Natl. Acad. Sci. USA 1992, 89, 10578. [PubMed: 1359541]

[17]. Wen AM, Lee KL, Yildiz I, Bruckman MA, Shukla S, Steinmetz NF, J. Vis. Exp 2012, 69, e4352.

[18]. Dakappagari NK, Lute KD, Rawale S, Steele JT, Allen SD, Phillips G, Reilly RT, Kaumaya PT, J. Biol. Chem 2005, 280, 54. [PubMed: 15507452]

[19]. Chatterji A, Ochoa WF, Paine M, Ratna BR, Johnson JE, Lin T, Chem. Biol 2004, 11, 855. [PubMed: 15217618]

[20]. Andreasson K, Tegerstedt K, Eriksson M, Curcio C, Cavallo F, Forni G, Dalianis T, Ramqvist T, Int. J. Cancer 2009, 124, 150. [PubMed: 18839427]

[21]. Occhipinti S, Sponton L, Rolla S, Caorsi C, Novarino A, Donadio M, Bustreo S, Satolli MA, Pecchioni C, Marchini C, Amici A, Cavallo F, Cappello P, Pierobon D, Novelli F, Giovarelli M, Clin. Cancer Res. 2014, 20, 2910. [PubMed: 24668647]

[22]. a)Azvolinsky A, JNCI, J. Natl. Cancer Inst. 2013, 105, 248; [PubMed: 23369950] b)Winter H, Fox BA, Ruttinger D, Methods Mol. Biol 2014, 1139, 555; [PubMed: 24619704] c)Melero I, Gaudernack G, Gerritsen W, Huber C, Parmiani G, Scholl S, Thatcher N, Wagstaff J, Zielinski C, Faulkner I, Mellstedt H, Nat. Rev. Clin. Oncol 2014, 11, 509. [PubMed: 25001465]

[23]. a)Ross JS, Fletcher JA, Oncologist 1998, 3, 237; [PubMed: 10388110] b)Weigelt B, Peterse JL, van ‘t Veer LJ, Nat. Rev. Cancer 2005, 5, 591. [PubMed: 16056258]

[24]. O’Sullivan CC, Smith KL, Curr. Breast Cancer Rep. 2014, 6, 169. [PubMed: 25285186]

[25]. Patel R, Czapar AE, Fiering S, Oleinick NL, Steinmetz NF, ACS Omega 2018, 3, 3702. [PubMed: 29732445]

[26]. Kennedy R, Celis E, Immunol. Rev 2008, 222, 129. [PubMed: 18363998]

[27]. Bennett SR, Carbone FR, Karamalis F, Flavell RA, Miller JF, Heath WR, Nature 1998, 393, 478. [PubMed: 9624004]

[28]. Williams MA, Tyznik AJ, Bevan MJ, Nature 2006, 441, 890. [PubMed: 16778891]

[29]. Shedlock DJ, Shen H, Science 2003, 300, 337. [PubMed: 12690201]

[30]. Braun M, Jandus C, Maurer P, Hammann-Haenni A, Schwarz K, Bachmann MF, Speiser DE, Romero P, Eur. J. Immunol 2012, 42, 330. [PubMed: 22057679]

[31]. Datta J, Rosemblit C, Berk E, Showalter L, Namjoshi P, Mick R, Lee KP, Brod AM, Yang RL, Kelz RR, Fitzpatrick E, Hoyt C, Feldman MD, Zhang PJ, Xu S, Koski GK, Czerniecki BJ, OncoImmunology 2015, 4, e1022301. [PubMed: 26451293]

[32]. a) Xie Y, Chen Y, Ahmed KA, Li W, Ahmed S, Sami A, Chibbar R, Tang X, Tao M, Xu J, Xiang J, Cancer Gene Ther. 2013, 20, 590; [PubMed: 24052129] b) Melssen M, Slingluff CL Jr., Curr. Opin. Immunol 2017, 47, 85. [PubMed: 28755541]

[33]. a)Khalil DN, Smith EL, Brentjens RJ, Wolchok JD, Nat. Rev. Clin. Oncol 2016, 13, 273; [PubMed: 26977780] b)Lee KL, Murray AA, Le DHT, Sheen MR, Shukla S, Commandeur U, Fiering S, Steinmetz NF, Nano Lett. 2017, 17, 4019. [PubMed: 28650644]

[34]. a)Betting DJ, Yamada RE, Kafi K, Said J, van Rooijen N, Timmerman JM, J. Immunother 2009, 32, 622; [PubMed: 19483647] b)Houot R, Kohrt HE, Marabelle A, Levy R, Trends Immunol. 2011, 32, 510; [PubMed: 21907000] c)Stagg J, Loi S, Divisekera U, Ngiow SF, Duret H, Yagita H, Teng MW, Smyth MJ, Proc. Natl. Acad. Sci. USA 2011, 108, 7142. [PubMed: 21482773]

[35]. a)Lebel ME, Chartrand K, Tarrab E, Savard P, Leclerc D, Lamarre A, Nano Lett. 2016, 16, 1826; [PubMed: 26891174] b)Lizotte PH, Wen AM, Sheen MR, Fields J, Rojanasopondist P, Steinmetz NF, Fiering S, Nat. Nanotechnol 2016, 11, 295. [PubMed: 26689376]

[36]. Dakappagari NK, Pyles J, Parihar R, Carson WE, Young DC, Kaumaya PT, J. Immunol 2003, 170, 4242. [PubMed: 12682258]

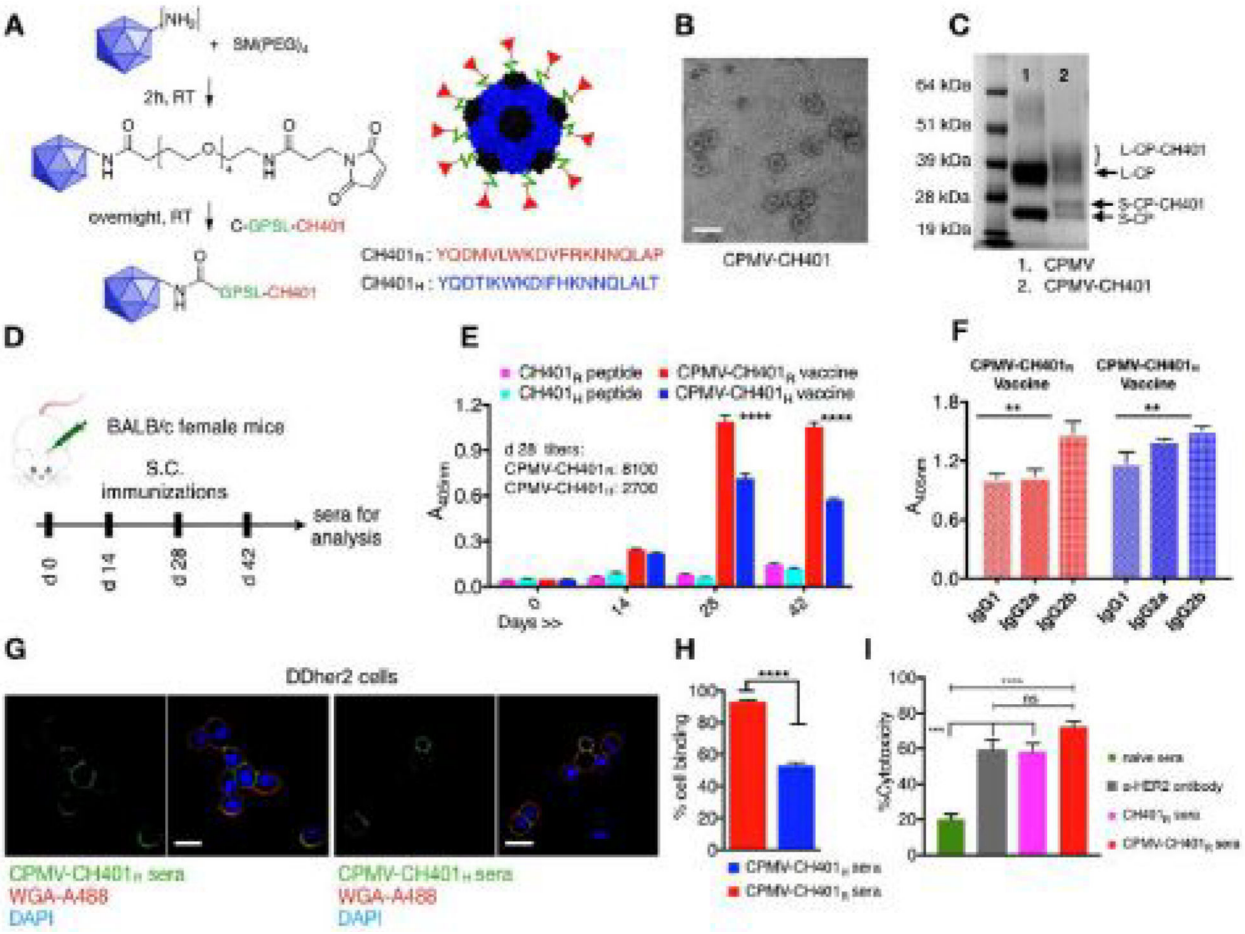

Figure 1.

Synthesis and characterization of CPMV-CH401 vaccine and measure of immunogenicity. A) CH401 peptide (rat or human) designed with a flexible GPSL linker and a terminal cysteine residue was conjugated to lysine residues of CPMV capsid via a hetero bi-functional N-hydroxysuccinimide-PEG4-maleimide (SM-PEG4) linker using a two-step process resulting in a multivalent vaccine. B) TEM imaging shows intact CPMV-CH401 particles post purification; the scale bar is 50 nm. C) SDS gel electrophoresis was used to confirm and quantify CH401 peptide conjugation on CPMV capsid consisting of small coat proteins (S-CP, 24 kDa) and large coat protein (L-CP, 42 kDa). The modified coat proteins are indicated as S-CP-CH401 and L-CP-CH401. D) Immunization schedule used for female Balb/c mice; sera were collected before and after immunization; vaccine variants CPMV-$CH401_H$ containing the human CH401 peptide (blue) ($n = 9$) and its rat homologue CPMV-$CH401_R$ (red) ($n = 10$) were tested along with soluble $CH401_H$ ($n = 10$) and soluble $CH401_R$ ($n = 10$). E) ELISAs were performed using pooled sera (at 1:100 dilutions) in triplicates, to determine rat CH401-specific antibody titers generated by CPMV-CH401 formulations versus free peptides. F) Anti-HER2 IgG isotypes were compared between the pooled sera (at 1:100 dilutions) of CPMV-$CH401_R$ (red bars) versus CPMV-$CH401_H$ (blue bars) using ELISAs on a recombinant HER2 coated plate (in triplicates). G,H) Confocal microscopy and flow cytometry (each sample tested in triplicates) was used to confirm the

binding of the pooled sera from the mice immunized with vaccine formulations to DDHER2 cells. The scale bar in G is 18 μm. Flow cytometry was analyzed using one-way ANOVA, ****$p < 0.0001$. I) MTT assays were used to compare complement-mediated cytotoxicity (CDC) of sera from immunized mice versus naïve mouse sera versus anti-HER2 antibody on DDHER2 cells (4 replicates per sample). Statistical analysis between various groups performed by two-way ANOVA using Tukeyyp multiple comparison (****$p < 0.0001$, ***$p < 0.001$, **$p < 0.01$, *$p < 0.05$, and ns = no significance).

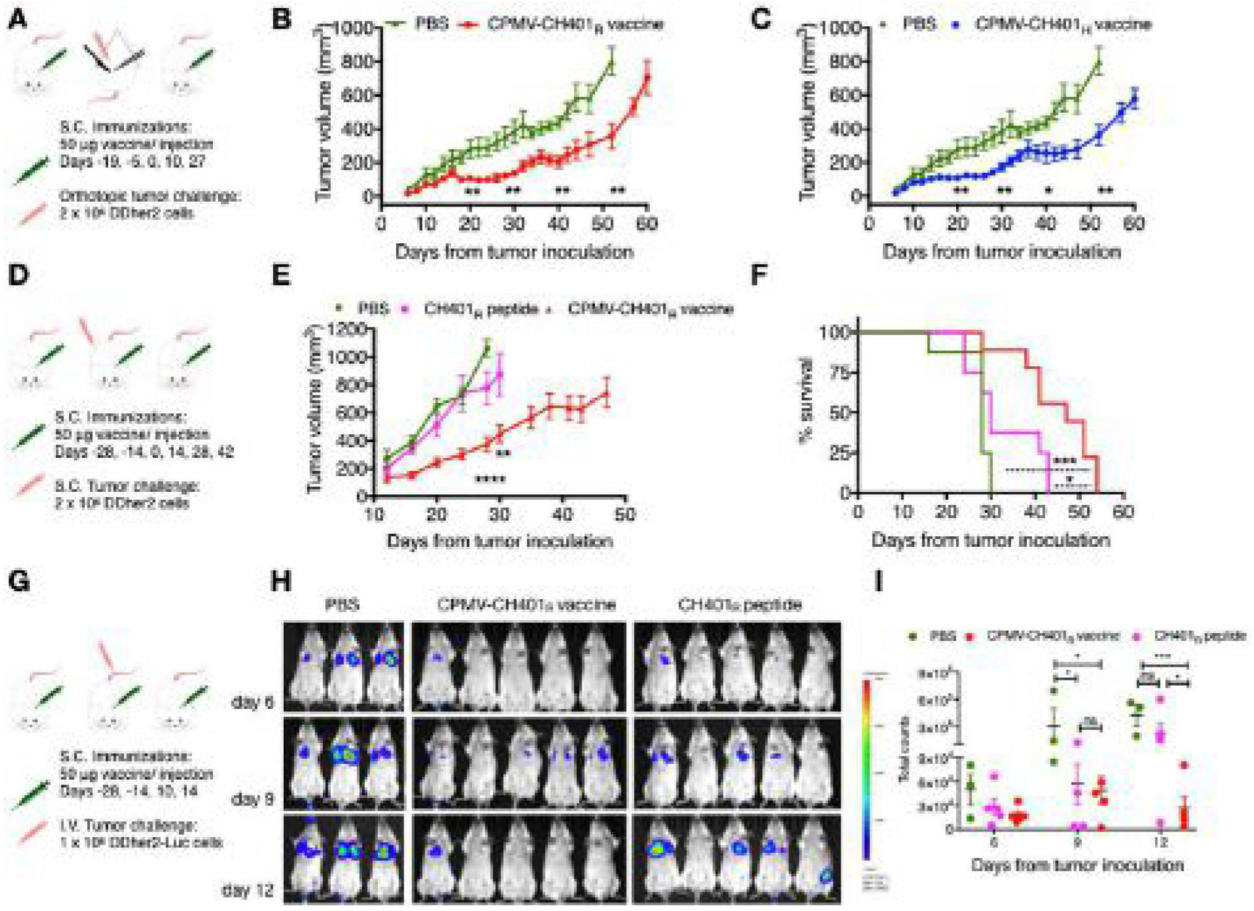

Figure 2.

CPMV-CH401 vaccine efficacy in Balb/c mice: A) Female Balb/c mice were challenged DDHER2 cells orthotopically through surgical inoculations in mammary fat pads following two immunizations and followed by two more immunizations. B,C) Mice immunized with CPMV-CH401$_R$ ($n = 10$) and CPMV-CH401$_H$ vaccines ($n = 9$) showed significantly slower tumor progression as compared to nonimmunized mice ($n = 10$) over a 60-day period. Data is plotted to day where $n \geq 5$ for each group. Statistical analysis between tumor volumes on days 20, 30, 40 and 55 was=performed using ordinary one-way ANOVA using Tukey's multiple comparison (***$p < 0.0001$, **$p < 0.01$, *$p < 0.05$). D) Subcutaneous DDHER2 tumors were grafted on day 28 following immunization with CPMV-CH401$_R$ vaccine, free peptide, or PBS and received 3 more doses subsequently. E) Tumor progression was monitored and data was plotted to day where $n \geq 5$. F) Overall survival benefit between the immunized and control group was compared using Kaplan–Meier plot. Statistical analysis on the survival curves was performed using Log-rank (Mantel–Cox) test (***$p < 0.001$). G,H) To model metastatic disease, DDHER2 cells were intravenously injected in mice immunized with CPMV-CH401$_R$ vaccine ($n = 5$), free peptide ($n = 5$) or PBS ($n = 3$) (schematic is shown in G). Bioluminescence imaging on IVIS Spectrum Imaging system was used to monitor tumor progression in lungs over time (days 6, 9, 12) (H), and regions of interest (ROI) measurements were performed using the Living Image Software for a semi-

quantitative analysis. Statistical analysis between treatment groups was performed using two-way ANOVA using Tukey's multiple comparison test (***$p < 0.001$, *$p < 0.05$).

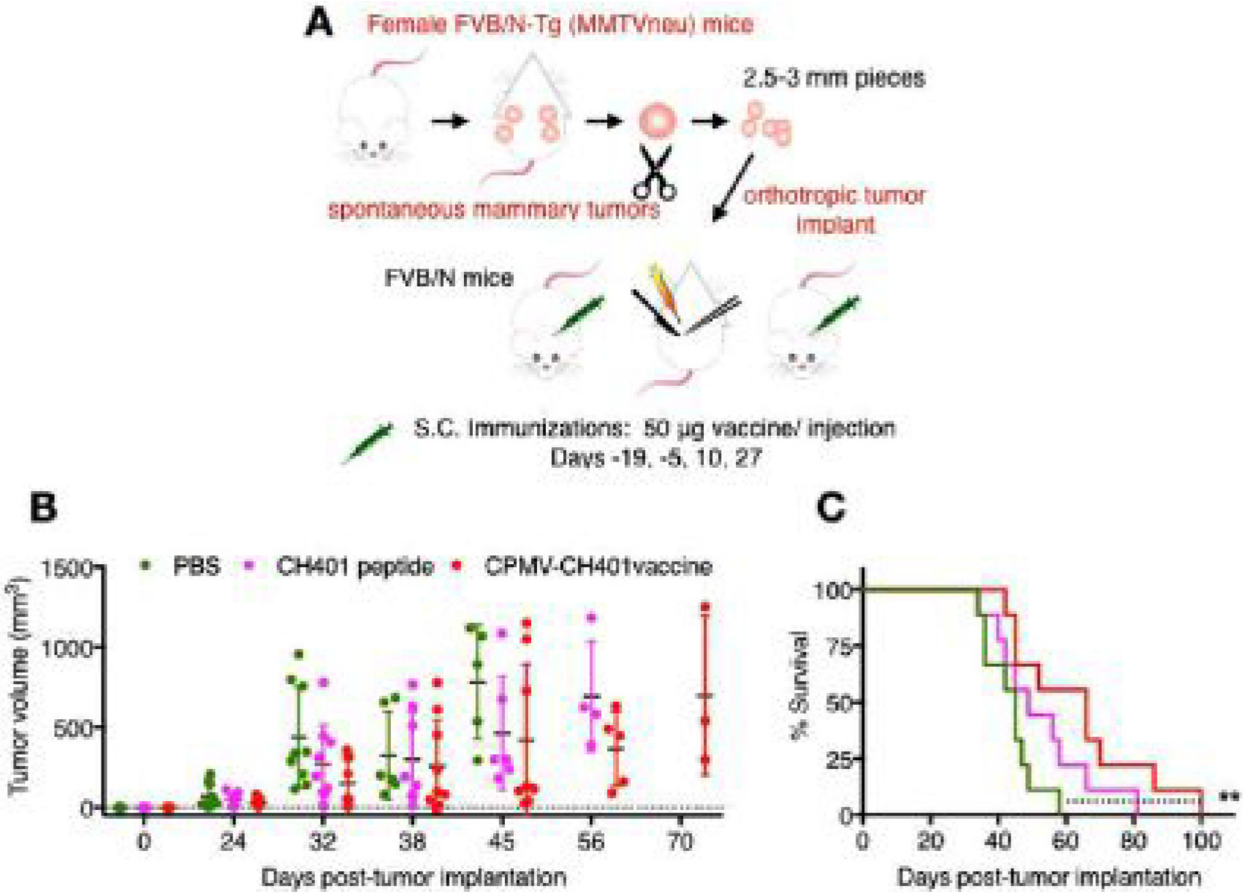

Figure 3.

Evaluation of CPMV-CH401 vaccine in a tumor transplant model: A) FVB/N female mice ($n = 10$) were immunized bi-weekly with four doses of vaccine or free peptide before and after tumor implantation. Tumors harvested from female FVB/N-Tg (MMTVneu) mice were chopped into small pieces and were transplanted into the mammary fat pads of immunized and control FVB/N females and tumor growth monitored. B) Comparative tumor volumes on multiple days (to $n \geq 3$) revealed the vaccine consistently slowed tumor progression compared to peptide immunized and control mice. Statistical analysis between the tumor volumes on individual days was performed using student *t*-test (**$p < 0.005$, *$p < 0.05$). C) Kaplan–Meier plot comparing the survival benefits offered by the vaccine over control mice. Statistical analysis on the survival curves was performed using Log-rank (Mantel–Cox) test (**$p < 0.01$).

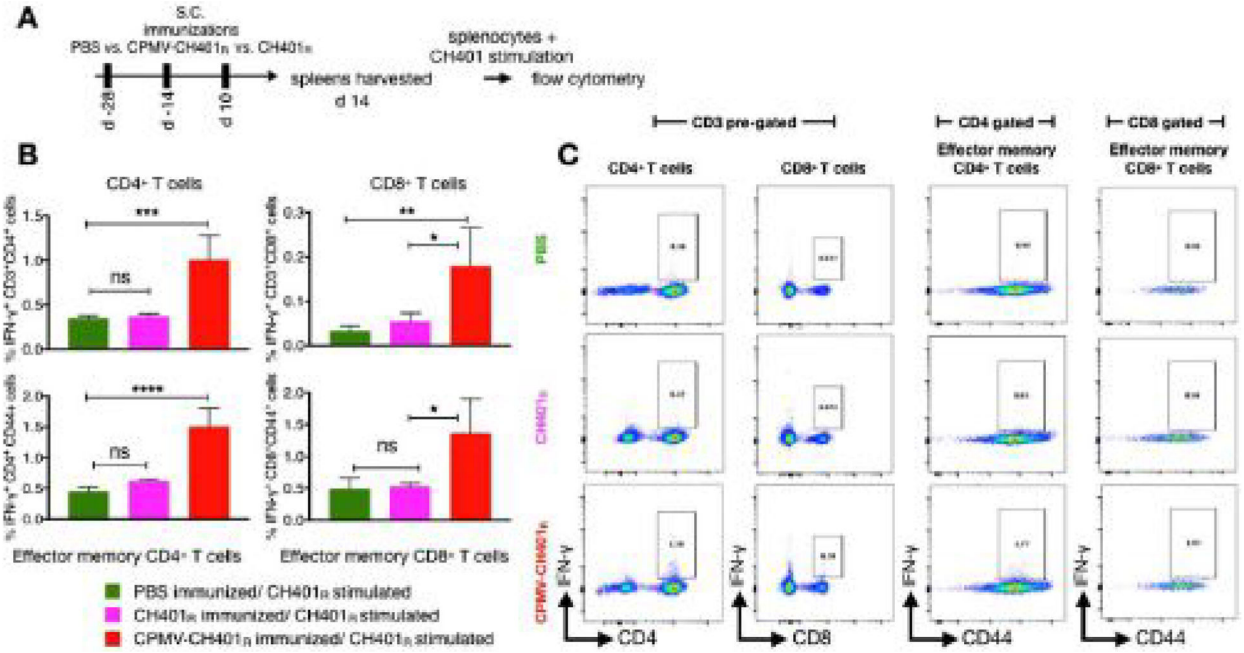

Figure 4.

Flow cytometry analysis: A) Splenocytes isolated from immunized mice ($n = 5$) were ex vivo stimulated with CH401 peptide and stained for intracellular IFN-γ. B and C) Cells were characterized as $CD4^+$, $CD8^+$ T cells, and effector memory $CD4^+$, $CD8^+$ T cells. Averages of triplicates with standard deviation are shown; statistical analysis was performed by one-way ANOVA using Tukey's multiple comparison test with, $^{**}p < 0.005$, $^{*}p < 0.05$.

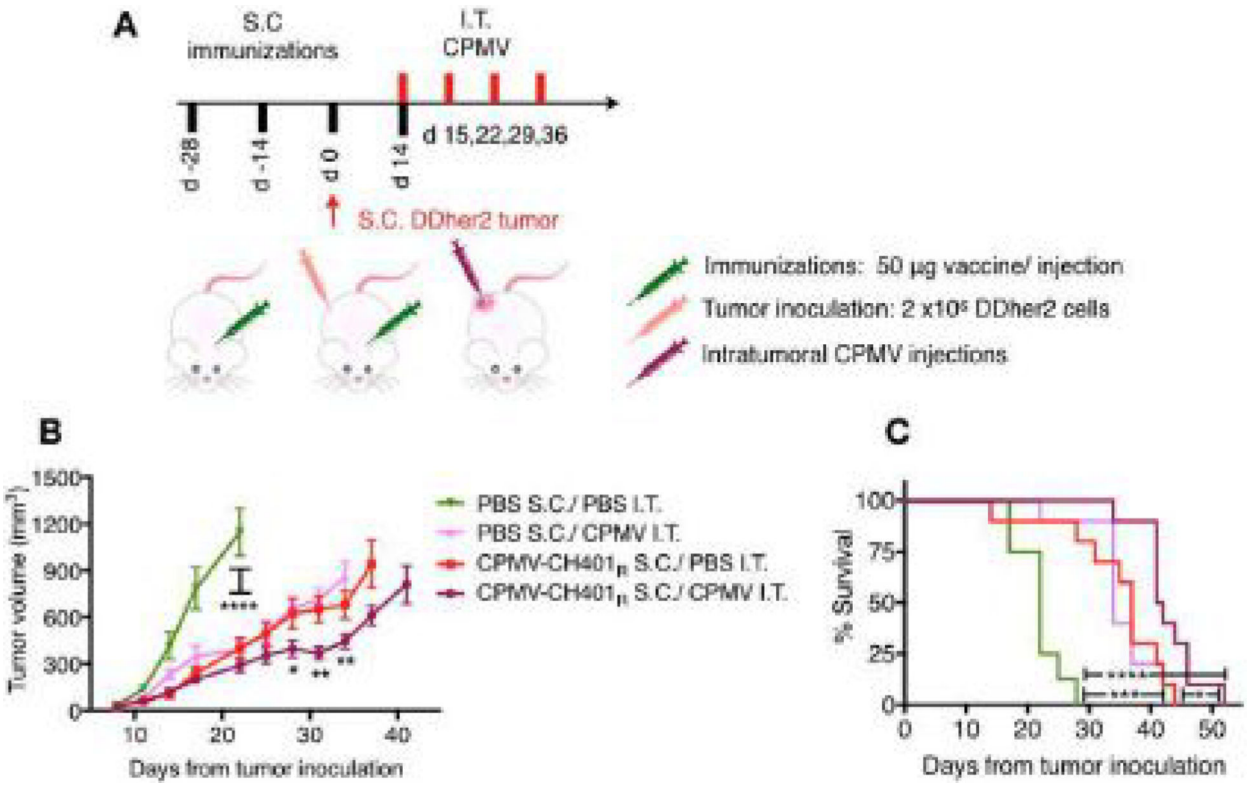

Figure 5.

Combining CPMV-CH401 vaccine with in situ vaccination with CPMV. A) A combinatorial approach was tested where CPMV-CH401 immunized mice ($n = 10$) grafted with subcutaneous DDHER2 tumors were also treated with four weekly doses of intratumoral CPMV injections. B) Tumor growth was monitored between control untreated mice ($n = 8$) and mice receiving CPMV-CH401 immunizations ($n = 10$), CPMV in situ vaccination ($n = 10$), or a combination of both ($n = 10$). Tumor volumes were plotted to days where $n \geq 5$. Statistical analysis was performed by ordinary one-way ANOVA using Tukey's multiple comparison tests (****$p < 0.0001$, **$p < 0.001$, *$p < 0.01$). C) Kaplan–Meier plot compares the survival benefits offered by combination therapy over monotherapy and no treatment. Statistical analysis on the survival curves was performed using Log-rank (Mantel–Cox) test (****$p < 0.0001$; ***$p < 0.001$, *$p < 0.05$).